Journal of Alloys and Compounds, 182 (1992) 243–252
JALCOM 120

A transmission electron microscopy and differential thermal analysis study of the ZrCo–H system

T. Schober and J. Friedrich
Institut für Festkörperforschung, Forschungszentrum, 517 Jülich (FRG)

(Received September 9, 1991; in final form September 12, 1991)

Abstract

ZrCo has been suggested as a storage medium with rather low equilibrium pressures for hydrogen and its isotopes. Here, the system ZrCo–H was investigated with conventional transmission electron microscopy and differential thermal analysis techniques. Hydrogen charging of ZrCo samples was mainly achieved by exposure to orthophosphoric acid. The β-hydride phase of composition $ZrCoH_3$ was found to precipitate on {100}. The orientation relationship of β with the matrix was established. The selected area diffraction results confirm the reciprocal lattice derived from the structure proposed by Irodova *et al.* in 1978. Low temperature phase transitions were not detected. DTA curves obtained from $ZrCoH_3$ powder produced from the gas phase display an endothermic peak between 320 and 340 °C which is due to an outgassing reaction. Bulk samples display another peak near 490 °C which is tentatively ascribed to the phase transition: ordered β-phase → disordered α-phase. A phase diagram for the pseudo binary phase ZrCo–H is proposed.

1. Introduction

ZrCo has been discussed recently as a low equilibrium pressure storage material for hydrogen and its isotopes, notably the isotope tritium [1–8]. When compared with the usual material for storing tritium uranium, ZrCo has the advantages of not being pyrophoric, radioactive and difficult to obtain. Among its disadvantages, however, when compared with uranium we list the possibility of long-term disproportionation, the higher vapour pressure at ambient temperature and the somewhat slower kinetics [7]. For a review of various storage compounds with low equilibrium pressures and a presentation of van't Hoff plots for these alloys see ref. 5. Here, we present the results of a transmission electron microscopy (TEM) and differential thermal analysis (DTA) study on ZrCo hydrides. Some of these results were also presented in a recent internal report [9].

2. Experimental details

2.1. Sample preparation

Ingots of ZrCo were produced by induction melting in a cold crucible under about 1 bar of highest purity argon gas purified by additional getters.

0925-8388/92/$5.00

The starting purity of the elements was three-to-four nines. The solidified ZrCo ingots were turned over and remelted several times for purposes of homogeneity. The ingots were then given a final high vacuum anneal at about 10^{-4} Pa and 950 °C for 48 h.

Slicing the ingots to sheets roughly 400 μm thick was carried out either by spark cutting or with a diamond wire saw. From these sheets, discs 3 mm in diameter were machined by spark erosion and these were subsequently ground to a thickness of about 150 μm. Further vacuum degassing at 10^{-5} Pa and 700 °C was then carried out. With regards to the TEM preparation, the best results were obtained with a two-stage electropolishing procedure. First, the samples were jet polished in a Tenupol unit using an electrolyte of 590 ml of methanol, 350 ml of butyl glycol and 60 ml of perchloric acid at −20 °C and a current of about 70 mA. Subsequently, the perforated samples were polished for about 2 s in a stationary electrolyte of 60 ml methanol, 36 ml butyl glycol and 6 ml of perchloric acid at about 20 V and −40 °C. We routinely obtained perfectly electropolished ZrCo samples.

2.2. Hydriding of ZrCo

It was found possible either to hydride prethinned ZrCo samples, or else to use gas-phase charged hydrides with only a small hydrogen concentration. No attempt was made in this work to investigate hydrided ZrCo powder by TEM.

Hydriding of prethinned ZrCo samples was achieved by immersing the samples in concentrated orthophosphoric acid at 55 °C for a time span of between 1 and 10 min. A 10 min exposure will cause complete surface hydriding of the sample. Thus the transparent areas will be exclusively in the hydride phase. Cursory experiments showed that the hydriding can also be done electrolytically in dilute sulphuric acid. Deuterides can be produced by using D_3PO_4.

Bulk samples of $ZrCoH_{0.03}$ for subsequent TEM inspection and bulk samples of composition $ZrCoH_{1.3}$ for DTA experiments were produced by conventional gas-phase charging at 600 °C and slow cooling. The former two-phase TEM samples could be electropolished as described above for ZrCo. DTA was carried out in a Dupont model 1090 thermal analyser.

3. Results

The results are listed here in numerical order for the various samples.

3.1. Virgin ZrCo samples

(1) The ZrCo samples produced in this laboratory were surprisingly free from foreign phases such as $ZrCo_2$, Zr_2Co and oxides.

(2) Even after degassing at 700 °C small hydride platelets (Fig. 1) could be observed in the ZrCo samples. These platelets have the appearance of dislocation loops, lie on {100} planes and can be assigned an effective Burgers

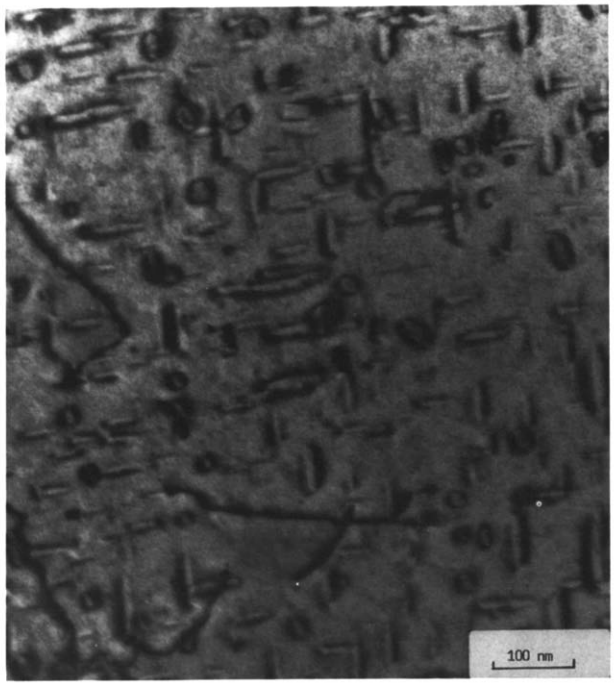

Fig. 1. TEM micrograph of "degassed" ZrCo: dislocation loop-like defects visible are thin hydride platelets of the β-phase ($ZrCoH_3$); habit plane {100}; 3 variants are visible.

vector $\boldsymbol{b}_{\text{eff}}$. The platelets become invisible when $\boldsymbol{g}\cdot\boldsymbol{b}_{\text{eff}}=0$. From contrast experiments we deduce that $\boldsymbol{b}_{\text{eff}} \| \langle 100 \rangle$. A schematic drawing of such a dislocation-loop-like hydride platelet is shown in Fig. 2.

3.2. ZrCo hydrogen-charged in H_3PO_4

(3) Exposure times of 1–2 min led to the formation of individual surface hydride patches as shown in Fig. 3. In the figure the protrusion of the particle into the hole is evidence that the hydride was formed after electropolishing.

(4) Using such two-phase regions the following orientation relationship between the hydride and the matrix M was obtained:

$$(001)_{\text{M}} \| (200)_{\text{hydride}} \qquad \text{and} \qquad [110]_{\text{M}} \| [020]_{\text{hydride}}$$

(5) Exposure for between 2 and 10 min led in most cases to complete surface hydriding to a depth of several hundred nm. The effects of corrosion were clearly visible: holes had formed and some surface material was dissolved. Fortunately, warm orthophosphoric acid was found to be more a chemical polishing than an etching solution. A typical micrograph is shown in Fig. 4. Here, the whole area is in the hydride phase. Domains of the ordered orthorhombic hydride phase are visible. Such areas are ideally suited for a diffraction analysis of the hydride.

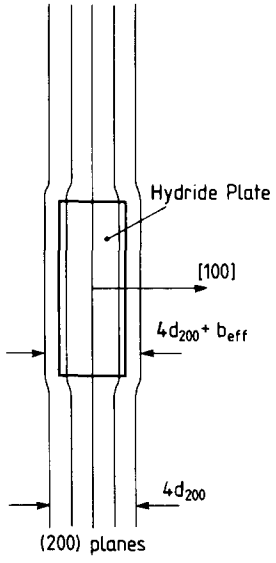

Fig. 2. Schematic model of a hydride platelet in ZrCo: similar to a dislocation loop of interstitial character with a Burgers vector $\boldsymbol{b}_{\text{eff}}$ which is the usual closure failure.

Fig. 3. TEM micrograph of a twinned particle of the β-hydride phase in ZrCo produced by immersing the prethinned ZrCo sample in warm orthophosphoric acid: the hydrided part protrudes into the hole.

3.3. ZrCo charged from the gas phase

(6) In Fig. 5 a typical area of ZrCo which has been gas-phase charged to the composition $ZrCoH_{0.03}$ is shown. Here, larger hydride plates are visible. In general, in low concentration gas-phase charged samples similar morphologies were observed as in chemically charged ZrCo.

3.4. Diffraction results

(7) In Fig. 6 a series of SAD patterns from essentially single domains of the hydride phase are presented. These patterns are fully compatible with the reciprocal lattice in Fig. 7 derived from the structure proposed in ref. 1. Furthermore, the absolute lattice parameters derived from our SAD results are in agreement with the data in ref. 1. Thus $ZrCo_3$ is isostructural with $ZrCoD_3$. So the general features of the structure proposed in ref. 1 are likely to be correct.

(8) A search for low temperature phase transformations using SAD techniques between -150 °C and ambient temperature did not reveal any evidence for new low temperature hydride phases arising from the possible ordering of hydrogen sublattice vacancies. Such transitions are commonly observed in other systems [10].

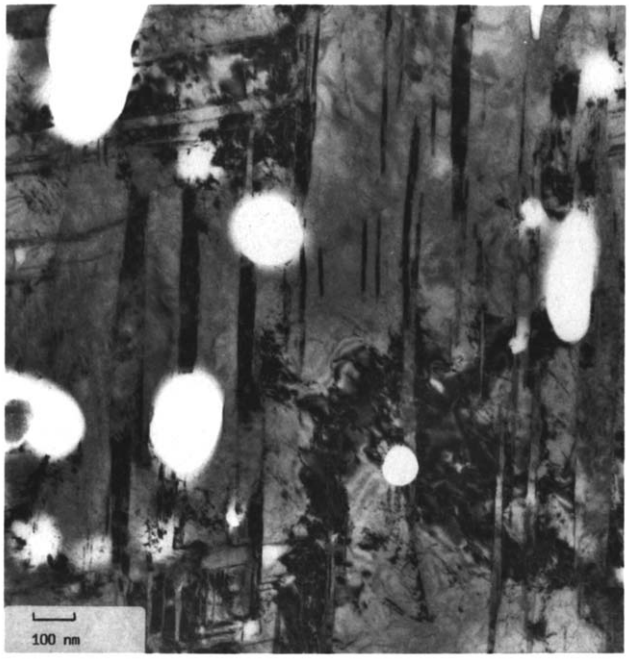

Fig. 4. TEM micrograph of a fully hydrided surface region: several single crystal hydride domains are visible separated by domain boundaries; holes are produced by the corrosive action of the acid.

3.5. Differential thermal analysis

(9) The main observation using gas-phase charged ZrCo–H powder was of an endothermic peak (Fig. 8(a)) located between 320 and 340 °C. On subsequent cooling no peak was observable.

(10) In contrast, in DTA runs two-phase solid bulk pieces of composition $ZrCoH_{1.3}$ displayed, in addition to the above peak between 320 and 340 °C, a second peak roughly located at 490 °C (Fig. 8(b)).

(11) DTA runs in flowing argon gas using powdered samples of $ZrCoH_x$ as produced by acid charging in H_3PO_4 also resulted in two similar DTA peaks in the ranges 320–340 °C and 480–500 °C. These peaks were, however, of an exothermic nature.

(12) DTA runs between −160 °C and ambient temperature did not display any evidence for low temperature hydride phase transitions.

4. Discussion

As in several other b.c.c. systems, precipitation occurs here on {100}. This apparently minimizes the elastic energy increase during precipitation. The surprisingly small sizes of the hydrides when compared with those of other b.c.c. metals [8] may well be related to the low diffusivity of hydrogen in ZrCo. The orientation relationship between the hydride and the ZrCo matrix

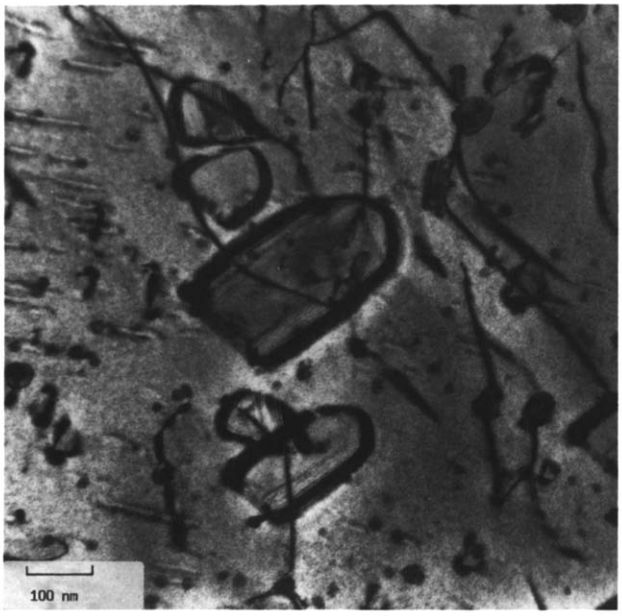

Fig. 5. TEM micrograph of larger hydride plates in a gas-phase charged ZrCo sample of composition $ZrCoH_{0.03}$.

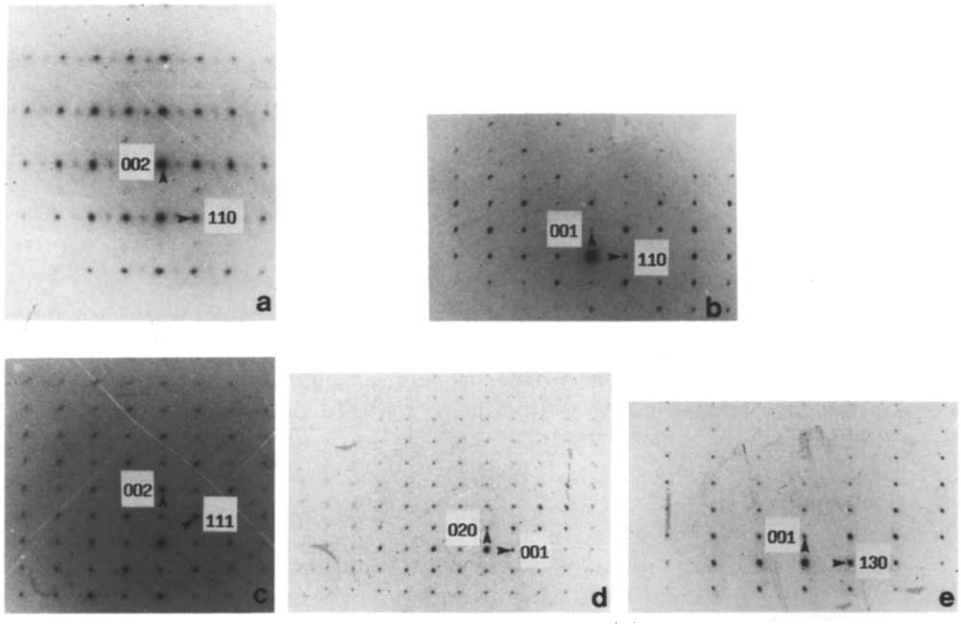

Fig. 6. SAD patterns of basically single domain areas of the β-hydride phase: all patterns represent planar sections of the model in Fig. 7; (apparent superlattice reflections in (a) along [110] are not real and presumably arise from interference of a second domain).

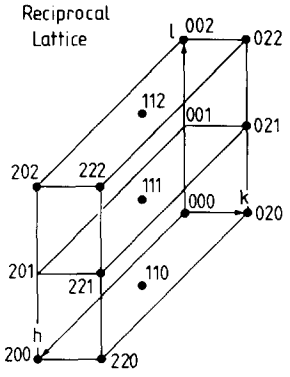

Fig. 7. Reciprocal lattice of $ZrCoD_3$ resulting from model proposed in ref. 1: lengths of unit vectors in reciprocal space roughly drawn to scale; systematic reflections absent in this figure may appear because of double diffraction.

is depicted in Fig. 9; details may be found in the figure caption. On the basis of this orientation relationship we propose the model illustrated in Fig. 9 for the atomic movements necessary to accomplish the phase transition

$$ZrCo + 1.5H_2 \longrightarrow ZrCoH_3$$

Neglecting small shifts in the horizontal direction the arrows in Figs. 9(a) and 9(b) denote the atomic shifts necessary to produce the hydride structure in Fig. 9(c). These shifts are not too extensive and do not apply to all the metal atoms.

Considering the hydrogen-induced lattice expansion, one unit cell of the hydride with four zirconium and four cobalt atoms having nominally 12 hydrogen atoms has a volume of 159.076×10^{-30} m^3, while the corresponding matrix unit cells each have a volume of 130.581×10^{-30} m^3, which constitutes a 22% volume increase. Assuming a realistic stoichiometry of $ZrCoH_{2.91}$ [6] rather than $ZrCoH_{3.0}$ we obtain a volume increase per hydrogen atom of

$$\Delta v \text{ per hydrogen atom} = 2.45 \times 10^{-30} \text{ m}^3$$

We may compare this with the rule of thumb by Peisl [11] stating that in many hydrides the space requirement for hydrogen amounts to about 2.9×10^{-30} m^3. Our value is about 15% below Peisl's average value. Unknown so far is the volume expansion of ZrCo in the dilute α-phase regime when hydrogen is added.

The various DTA observations can readily be rationalized in the following way. The peak between 320 and 340 °C is produced by an irreversible outgassing reaction. The associated enthalpy per gram is much too large for a hydride phase transition. We also note that the "internal" equilibrium hydrogen pressure of ZrCo hydride starts to exceed the external argon overpressure of 1 bar near 320 °C. This effect could prompt a outgassing reaction. An outgassing reaction between 320 and 340 °C would be accompanied by the formation of cracks and fissures in the samples. Given the

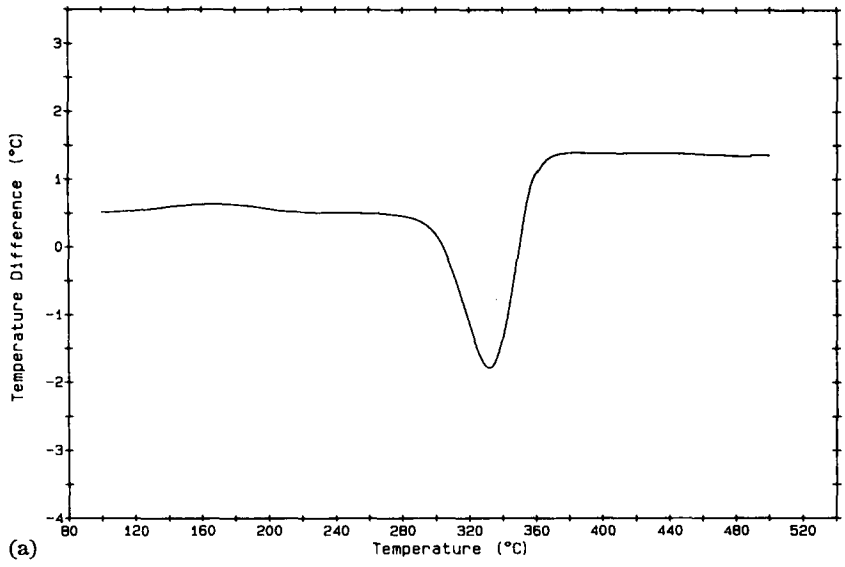

(a)

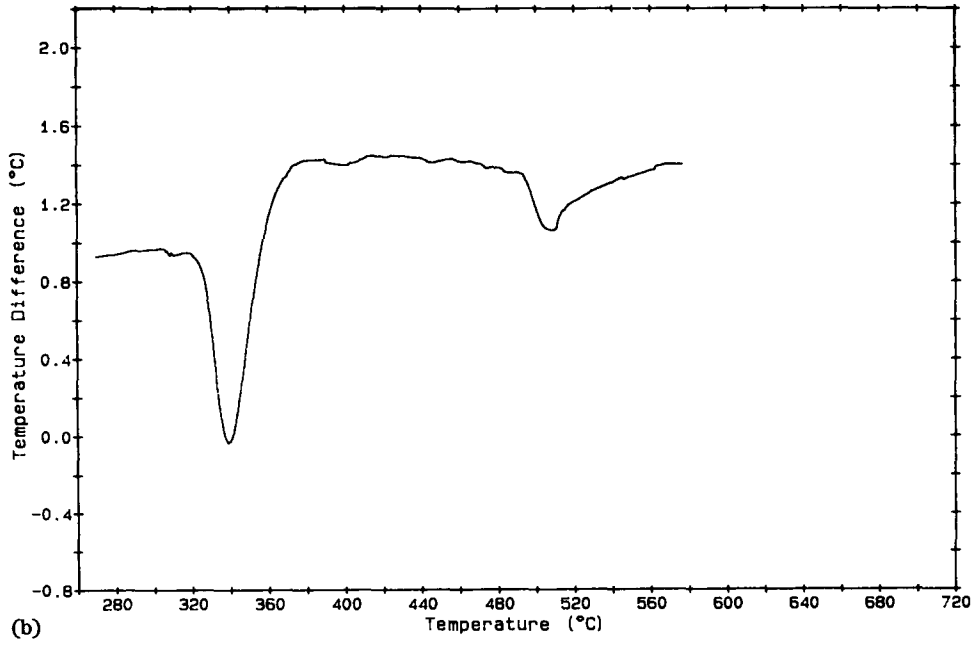

(b)

Fig. 8. DTA peaks in hydrided ZrCo samples: (a) endothermic peak in the range 320–340 °C obtained upon heating a sample of gas-phase charged $ZrCoH_3$ powder; heating rate 5 °C min^{-1}; the peak is caused by irreversible hydrogen loss from the sample; (b) endothermic peaks in bulk $ZrCoH_{1.3}$ in the ranges 320–340 °C and 480–500 °C; presumably, the first peak is produced by hydrogen loss, whereas the second peak is mainly due to the phase transition $\beta \rightarrow \alpha$; hydrogen loss is also expected to occur during the phase transition.

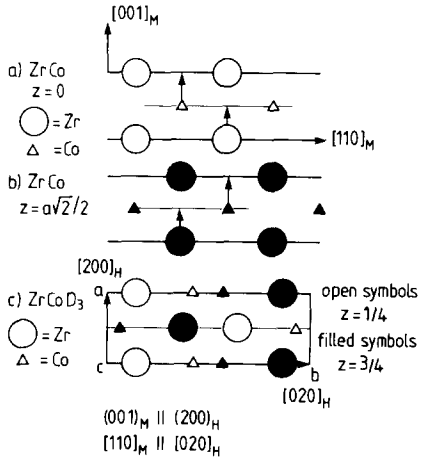

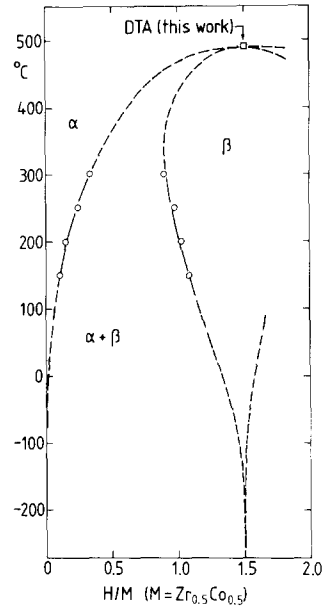

Fig. 9. Orientation relationship between matrix ZrCo and hydride $ZrCoH_3$: arrows denote major shifts necessary to transform the matrix to the hydride; (a) structure of ZrCo, $z = 0$; (b) structure of ZrCo, $z = \frac{1}{2}$; (c) structure of hydride or deuteride; hydrogen atoms are not shown.

Fig. 10. Pseudobinary ZrCo–H phase diagram proposed here: open circles, data taken from ref. 6; open square, DTA results, this work; details in text.

small grain size of the powder hydrided from the gas phase, all β-phase areas would be sufficiently close to a free surface for complete hydrogen loss to occur during the first DTA peak. We also assume that the surface chemistry of the gas-phase charged powder is conducive to rapid outgassing.

In contrast, the endothermic peak located near 490 °C is only observed in bulk samples with large diffusion distances. Here, the outgassing reaction between 320 to 340 °C was incomplete. The peak is attributed to the phase transition: ordered β-phase → disordered α-phase. Again, many cracks and fissures and considerable hydrogen loss would be a consequence of this phase transition.

The exothermic DTA peaks observed in acid-charged powder occur again in the temperature ranges 320–340 °C and 480–500 °C. We assume here that the argon gas used is slightly contaminated with oxygen and that fresh surfaces are formed during the outgassing reaction near 320–340 °C or during the phase transformation near 490 °C, and that these then react exothermically with trace oxygen thus producing exothermic peaks.

Using the *p–c–T* data from ref. 6, the above phase transition temperature of 490 °C and also experience from the determination of other metal–hydrogen phase diagrams, we present in Fig. 10 a schematic model of the pseudobinary ZrCo–H phase diagram. It has the following features: (a) there is only one hydride, the β-phase of composition $ZrCoH_3$; (b) β transforms to α in a first-

order phase transition at the congruent "melting" temperature of approximately 490 °C; (c) the solubility of hydrogen in the α-phase vanishes at $T \rightarrow 0$ K and (d) the stoichiometry in the β-phase locks in at $H/M = 1.5$ for $T \rightarrow 0$ K where M represents $Zr_{0.5}Co_{0.5}$.

Acknowledgments

We thank J. B. Condon, M. Beyss and H. Wenzl for assistance and discussions. Our thanks are also owed to Bruno Bischof for the expert DTA, DSC and TGA experiments on the ZrCo hydrides.

References

1 A. V. Irodova, V. A. Somenkov, S. Sh. Shil'shtein, L. N. Padurets and A. A. Chertkov, *Sov. Phys.–Crystallogr., 23* (1978) 591.
2 S. J. C. Irvine and I. R. Harris, in A. F. Andresen and A. J. Maeland (eds.), *Hydrides for Energy Storage*, Pergamon, Oxford, 1978.
3 S. J. C. Irvine, D. K. Ross, I. R. Harris and J. D. Browne, *J. Phys. F, 14* (1984) 2881.
4 T. Nagasaki, S. Konishi, H. Katsuta and Y. Naruse, *Fusion Technol., 9* (1986) 506.
5 R.-D. Penzhorn, M. Devillers and M. Sirch, *J. Nucl. Mater., 170* (1990) 217.
6 M. Devillers, M. Sirch, S. Bredendink-Kämper and R.-D. Penzhorn, *Chem. Mater., 2* (1990) 255.
7 W. T. Shmayda, A. G. Heicz and N. P. Kherani, *J. Less-Common Met., 162* (1990) 117.
8 J. G. Dillard, H. Glasbrenner, G. Pfennig, H. Kleve-Nebenius and H. J. Ache, *J. Less-Common Met., 166* (1990) 233.
9 T. Schober and J. Friedrich, *Jül-Rep. 2503*, 1991 (Forschungszentrum Jülich).
10 T. Schober and H. Wenzl, in G. Alefeld and J. Völkl (eds.), *Topics in Applied Physics, Hydrogen in Metals II*, Vol. 29, Springer, 1978.
11 H. Peisl, in G. Alefeld and J. Völkl (eds.), *Topics in Applied Physics, Hydrogen in Metals I*, Vol. 28, Springer, 1978.